Formation and Characterization of Self-Assembled Films of Sulfur-Derivatized Poly(methyl methacrylates) on Gold

T. J. Lenk,† V. M. Hallmark, and J. F. Rabolt*

IBM Research Division, Almaden Research Center, 650 Harry Road, San Jose, California 95120-6099

L. Häussling and H. Ringsdorf

Institute for Organic Chemistry, University of Mainz, J. J. Becher Weg 22, D-6500 Mainz, Germany

Received July 6, 1992; Revised Manuscript Received October 26, 1992

ABSTRACT: Poly(methyl methacrylate) copolymers containing sulfide-derivatized side chains have been synthesized, and their adsorption onto gold has been characterized using ellipsometry, X-ray photoelectron spectroscopy, contact angle, and infrared measurements. The film thickness obtained by spontaneous adsorption of these polymers from solution was found to be a function of solution concentration and the spacing of the derivatized side chains along the backbone. Probing these films by secondary exposure to a semifluorinated *n*-alkyl thiol reveals that fluorocarbon domains form readily on the gold surface, although films of the polymer with side chains every 10 repeat units are resistant to displacement. A 24-Å layer of this polymer is able to completely shield the presence of a significant fluorocarbon layer during contact angle measurements.

Introduction

The interaction of polymers with surfaces and interfaces provides simultaneously an opportunity and a challenge: the former because it is now possible to control polymer architecture and hence to specify the function of a surface or interface through polymer adsorption and organization; the latter because the techniques commonly used in the study of thin films (e.g., infrared (IR), X-ray photoelectron spectroscopy (XPS), and scanning tunneling microscopy (STM)) must be pushed to record levels of sensitivity to investigate molecular orientation and order in monolayers. Progress toward these goals has been steady but slow.

Interest in self-assembly of polymers has been heightened by the large volume of work on short-chain thiols, which have been shown to form stable, well-organized, tightly-bound organic monolayers.[1-4] Self-assembled layers produced in this manner have been used in studies of wetting,[5] electrochemical reactions,[6,7] and model membranes.[8,9] The first extension of chemisorption to include sulfur-derivatized polymers was undertaken by McCarthy et al.[10] in their study of block copolymers of polystyrene–poly(propylene sulfide) on gold. Surface coverage measurements indicated that the sulfide-containing part of the polymer did indeed adsorb to the gold surface, forming a thin, strongly-bound film. Unfortunately, little information on the polymer topography on gold was given.

Using the ability to design polymers which contain multiple functionalities in the same chain, the present work addresses the adsorption of derivatized poly(methyl methacrylate) (PMMA) copolymers containing both side chain anchor (sulfide) and backbone spacer (methyl methacrylate) groups. The eventual goal of these studies is the formation of anchored polymer layers as shown in Figure 1, using the proper mix of anchor, extender, and specialized side chains to build controlled structures on metal surfaces. This paper will describe the effect of anchor side chain spacing on the orientation and topography of PMMA chains on gold using IR, XPS, contact angle, and ellipsometric measurements to investigate orientation, chemical composition, wetting properties, and thickness of the chemisorbed layers.

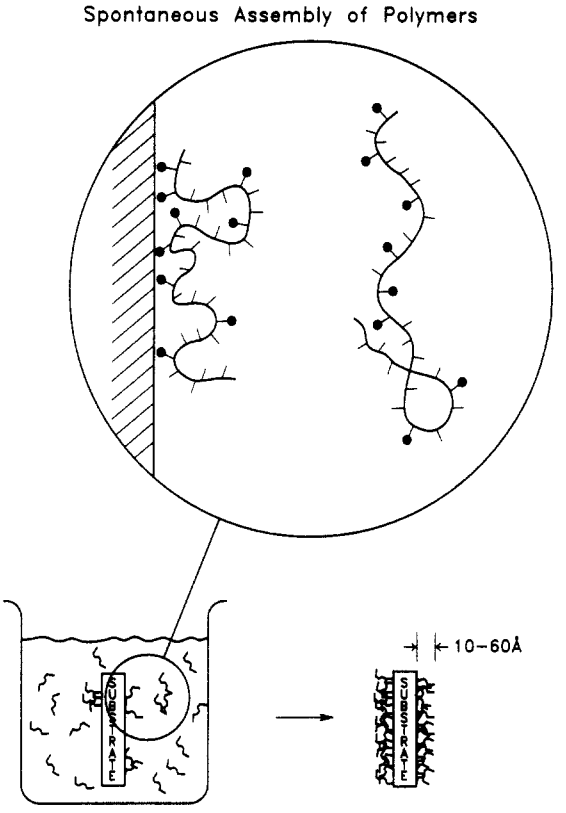

Figure 1. Formation of tethered polymer layers by spontaneous adsorption from solution.

Experimental Section

Copolymer Synthesis and Characterization. The polymers were synthesized by free-radical polymerization of methyl methacrylate (MMA) and 2-(methylthio)ethyl methacrylate (MTEMA) in toluene with azobis(isobutyronitrile) as a radical initiator at 60 °C, with subsequent precipitation from methanol and freeze-drying from benzene. The monomers were distilled and kept under argon in a freezer. Preparation of the monomeric sulfide (MTEMA) has been described previously.[11] Polymers

† Present address: Institute of Materials Science, U-136, University of Connecticut, Storrs, CT 06269.

0024-9297/93/2226-1230$04.00/0

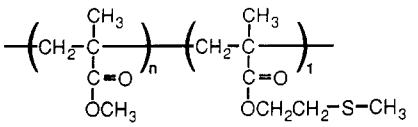

	n (monomer feed)	n (elemental analysis) polymer	M_w	M_n	S/Chain
PMMA-10	10	9.4	88,000	54,000	50-80
PMMA-100	100	100	81,000	37,000	5-10

Figure 2. Structure and composition of the two sulfide-derivatized PMMA polymers used in this work.

were synthesized using MMA:MTEMA ratios of 100:1 (PMMA-100) and 10:1 (PMMA-10) (see Figure 2). Elemental analysis reveals an MMA:MTEMA ratio of 100:1 for PMMA-100 (37% conversion) and 10:1.06 for PMMA-10 (30% conversion). The similarity of these ratios in the polymer to the monomer feed ratios is consistent with an essentially random incorporation of derivatized side chains into the polymer. Measured polydispersities were 1.6 and 2.2 for PMMA-10 and PMMA-100, respectively (see Figure 2). The notation S-PMMA will be used to refer generally to these materials in this paper.

Sample Preparation. Glass substrates (25 × 75 mm slides) were cleaned by an acid etch followed by degreasing in isopropyl alcohol vapor and drying under a warm nitrogen flow. Vacuum evaporation of 150 Å of chromium as an adhering layer was followed by evaporation of 2000 Å of gold. All depositions were done at a rate of 5–10 Å/s. Samples were immersed in solution within 1 h of removal from vacuum.

Gold substrates were placed in a solution of the polymer at room temperature for a specified time. Except for the kinetic experiments, adsorptions were for approximately 24 h. Most experiments described in this paper were conducted using methyl ethyl ketone, but similar results were observed with dichloromethane. Samples were rinsed copiously with the adsorption solvent upon removal from solution, blown dry with nitrogen, and then vacuum-dried at room temperature. No residual solvent bands appeared in the infrared spectra.

Analysis. All infrared measurements were made using an IBM/Bruker Model 98 evacuable FTIR at a resolution of 4 cm^{-1}. Typical spectra required the coaddition of 8000 scans to obtain a reasonable signal-to-noise ratio. All spectra of the adsorbed films on gold were recorded using grazing angle external reflection, so that only vibrations with a change in the component of their dipole moment normal to the surface are observed in the spectrum.[12,13] Transmission spectra of "bulk" material were recorded using cast films on KBr plates.

Advancing and receding water contact angles were measured using a Rame-Hart Model 100-00 goniometer and a syringe-driven droplet. X-ray photoelectron spectroscopy (XPS) measurements were made using a Surface Science Instruments SSX-100 Model 05 spectrometer with a monochromatic Al Kα source. Ellipsometric measurements were made on a Rudolph Research AutoEL ellipsometer using a 6328-Å laser at a 70° angle of incidence. A refractive index of 1.50 was assumed for thickness calculations, compared to values of 1.49 for poly(methyl methacrylate), 1.48 for poly(2-ethoxyethyl methacrylate), and 1.51 for poly(2-hydroxymethyl methacrylate).[14] Varying this value from 1.4 to 1.6 resulted in approximately a ±10% difference in the estimated thickness.

Results and Discussion

Underivatized PMMA. Gold surfaces, as prepared in vacuum, are hydrophilic in nature. Contamination of the gold surface by atmospheric hydrocarbons occurs rapidly, resulting in a hydrophobic surface with an advancing contact angle between 50 and 60° after 90 min.[15] Thus, for nominally clean gold substrates such as those used in this study, some small spontaneous adsorption of underivatized PMMA would be expected due to interactions of the polar methoxy and carbonyl groups with the hydrophilic surface.

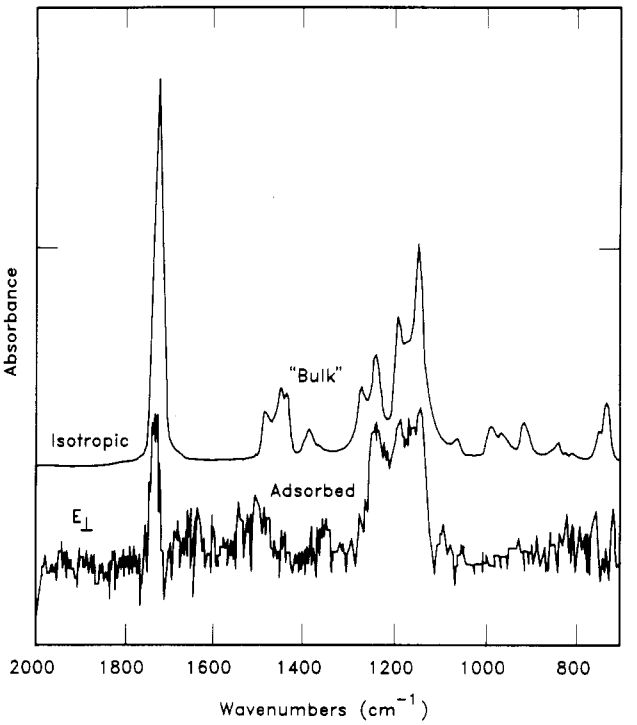

Figure 3. Comparison of a transmission infrared spectrum of PMMA on KBr to the grazing incidence reflection spectrum of an adsorbed film of PMMA on gold.

Experimentally, exposure of gold surfaces to a 0.1 mg/mL solution of underivatized PMMA resulted in an adsorbed polymer film of thickness <10 Å. Advancing and receding contact angles for this spontaneously adsorbed film were 68 and 55°, respectively, compared to 69 and 49° for a thick cast film of the same polymer. The similarity of the contact angles and hysteresis for the two films suggests that surface coverage for the spontaneously adsorbed film is relatively complete and homogeneous, at least on a lateral scale of microns.

Infrared spectroscopy can yield orientational information for adsorbed molecules, due to the selection rules for grazing incidence reflection on metals.[12] Interactions between incident and reflected infrared radiation cause only those vibrations which have dipole moment components normal to the metal surface to appear in the absorption spectrum. The spectrum for a bulk sample of PMMA[13,16] prepared as a cast film on a KBr substrate is shown in the upper trace of Figure 3. This isotropic spectrum is noticeably different from the spectrum of the adsorbed PMMA film on gold, shown in the lower trace of Figure 3. The ester C–O–C stretching region (1100–1300 cm^{-1}) is greatly enhanced relative to the carbonyl C=O stretch at 1740 cm^{-1}, indicating that the adsorbed film is highly oriented. The adsorbed PMMA film has a higher relative concentration of methoxy groups oriented normal to the metal surface as compared with carbonyl groups.

Derivatized PMMA. Although a very thin layer of underivatized PMMA adsorbs spontaneously from solution onto a gold surface, the addition of sulfur-derivatized side chains to the PMMA polymer should result in an increased adsorption to gold. The Au–S interaction is quite specific and is strong enough to result in self-assembly of highly-ordered monolayers of monomeric species such

Table I
Properties of S-PMMA Adsorbed Films[a]

	thickness (Å)	θ_{adv} (deg)	θ_{rec} (deg)
PMMA-10			
0.1 mg/mL	24 ± 3	64 ± 2	41 ± 3
0.001 mg/mL	16 ± 3	66 ± 2	45 ± 4
PMMA-100			
0.1 mg/mL	32 ± 5	68 ± 2	39 ± 3
0.001 mg/mL	14 ± 4	68 ± 3	42 ± 4

[a] Adsorbed films were formed during 24 h of solution exposure to gold. All values are the average of measurements on at least five independently prepared samples.

as *n*-alkyl thiols. For the sulfur-derivatized polymers (S-PMMA) studied here, a relatively low concentration of Au–S linkages will be available, and the dependence of polymer adsorption, orientation, and order upon this concentration has been investigated. This initial report compares the results from two polymers, PMMA-10 and PMMA-100, with nominally one sulfide per 10 and 100 monomer units, respectively (see Figure 2).

Concentration Dependence. Compared with underivatized PMMA, sulfur derivatization does indeed increase polymer adsorption onto gold. For adsorption from 0.1 mg/mL solutions, the underivatized PMMA yielded a film thickness of <10 Å, while PMMA-10 and PMMA-100 gave film thicknesses of 24 and 32 Å, respectively (see Table I). For a lower concentration solution, 0.001 mg/mL, substantially lower film thicknesses were measured by ellipsometry: 16 Å for PMMA-10 and 14 Å for PMMA-100. This concentration dependence points to the existence of important kinetic effects during adsorption of the derivatized polymers from solution. The details of these kinetics will be explored in a later section.

While the film thicknesses for the two polymers and two different concentrations vary, the advancing and receding contact angles are quite similar for all four preparations. All values in Table I are the averages of samples prepared on at least five different occasions, and the error bars indicate generally good reproducibility. The advancing contact angles are comparable to that of underivatized PMMA (~69°), although the contact angle for PMMA-10 is slightly lower. All the receding contact angles are significantly lower than that measured on the underivatized PMMA film (~49°), perhaps reflecting interactions of the sulfide side chain groups with the water droplet.

Comparisons of the grazing incidence infrared spectra of PMMA-100 and PMMA-10 films adsorbed from a 0.1 mg/mL solution (referred to hereafter as thick films) with transmission spectra of the respective cast films are shown in Figure 4. As mentioned earlier, the spectra of the bulk materials are isotropic, while the reflection spectra of the films are effectively polarized, showing contributions from the components of changes in dipole moment perpendicular to the gold surface. For PMMA-100 (Figure 4a) the relative intensities of the peaks are nearly the same in both the transmission and reflection spectra, indicating that there is little orientation in the adsorbed film. The relative intensities in the 1100–1300-cm^{-1} region are different in the two spectra, which is probably indicative of a difference in the distribution of ester conformations[13] between the adsorbed polymer and the bulk material on KBr due to steric constraints imposed in the adsorbed film. In general, this film appears to be a collection of random chains, with a few anchor points per chain to hold the molecule in place.

For PMMA-10 (Figure 4b), the intensities of the carbonyl stretch at 1740 cm^{-1} and the CH_2 bending vibration at 1460 cm^{-1} are slightly enhanced relative to

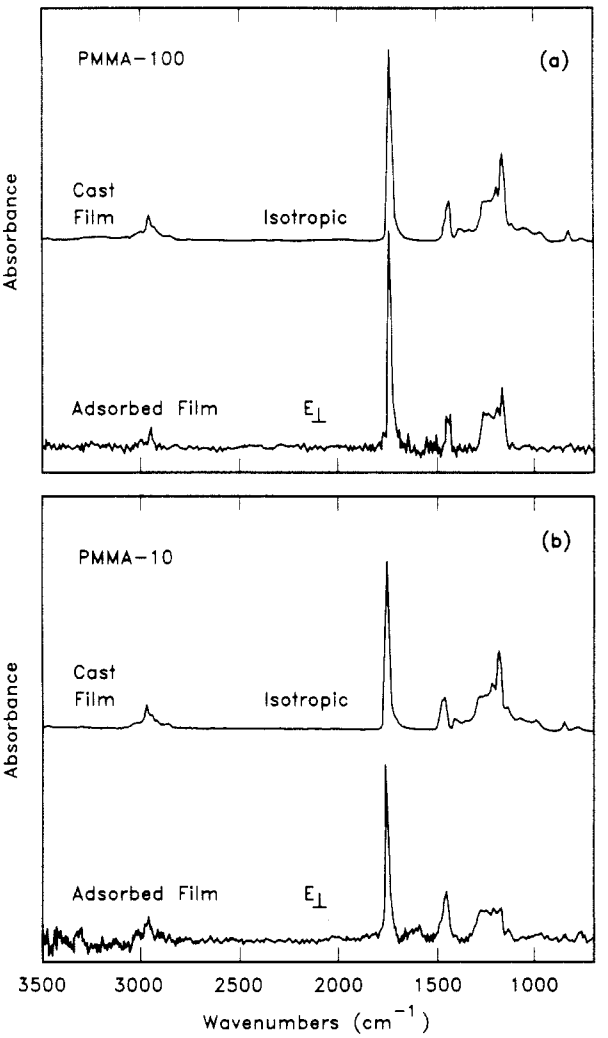

Figure 4. Comparison of the transmission infrared spectra of S-PMMA polymers in KBr to the grazing incidence reflection spectra of adsorbed films of these polymers on gold: (a) PMMA-100 (adsorbed film ~35 Å thick); (b) PMMA-10 (adsorbed film ~25 Å thick).

the C–O–C stretching region, indicating more orientation than in the PMMA-100 film. This is consistent with the fact that there are more attachment points along the chain in PMMA-10, which should result in more loops from the surface than in PMMA-100 and thereby a slightly higher degree of orientation. However, even this PMMA-10 film does not appear to be highly oriented compared to the underivatized PMMA shown in Figure 3. Again, the C–O–C stretching region changes to favor the higher wavenumber components (for both polymers), which may reflect the restrictive geometries available to the side chains in adsorbed films. Comparisons of these infrared spectra for thick films with those obtained for thinner films indicate that orientation within the self-assembled films does not depend upon film thickness or solution concentration, although the absolute absorptions do scale linearly as expected with film thickness.

It is clear that not all of the sulfide groups in PMMA-10 are interacting with the gold surface. First, the layer thickness for a film from a 0.1 mg/mL solution is about 24 Å. With sulfide side groups spaced approximately every 10 backbone units along the chain, this yields an average of 26 carbons and 2 oxygens between the sulfur atoms. Even folded into a tight loop with the sulfurs attached at adjacent sites, this would provide a thickness of only about 18 Å, smaller than the observed layer thickness. Second, the infrared data are not consistent with the high degree

Table II
Angular-Dependent XPS Measurements for a PMMA-10 Film[a]

	carbon	oxygen	sulfur
as adsorbed			
10°	69.7	29.2	1.2
70°	68.8	29.8	1.2
annealed			
10°	69.6	29.2	1.2
70°	68.2	30.5	1.4
bulk polymer	71.2	27.4	1.4

[a] Results have been normalized to correct for the differing amounts of gold seen in the spectrum due to different penetration depths of the X-ray beam. Angles are referenced to the surface normal. 10° values are more representative of the overall film composition, while 70° values are more representative of the vacuum–polymer interface.

of orientation that would be required for closely-packed stretched loops. This requires that the actual loops be much longer than the observed layer thickness, so that many of the sulfides must be away from the surface and distributed throughout the film. This picture is confirmed by X-ray photoelectron spectroscopy (XPS) of PMMA-10 films.

XPS measurements were made with the X-ray beam incident at 10 and 70° to the surface normal. The beam coming in at 70° will not penetrate as deeply beyond the interface, and the results will be more representative of the composition near the vacuum–polymer interface, while the overall film composition will be more represented by the 10° beam results.[17] As can be seen from Table II, there is no significant difference between measurements at the two different angles and no significant difference between the measured values and the actual polymer composition. This indicates that the sulfide groups are probably distributed relatively uniformly throughout the film, and certainly are not concentrated at the gold surface. A shift of approximately 3 eV in the sulfur $2p_{1/2}$ and $2p_{3/2}$ peaks should also be observed upon chemisorption of the sulfur to gold.[17] However, the polymer was observed to degrade in the X-ray beam, with loss of sulfur observed upon prolonged exposure. This prevented extended analysis, and because of the low signal-to-noise ratio and the overlap of the sulfur $2p_{1/2}$ and $2p_{3/2}$ peaks, it was impossible to clearly distinguish differences in the amount of chemisorbed sulfur for the different conditions. However, for all measurements reported here the compositions before and after analysis were as expected, particularly the carbon/sulfur ratio.

The composite microscopic structure of the adsorbed films as measured by ellipsometry, contact angles, infrared spectroscopy, and XPS is shown in Figure 5. Underivatized PMMA forms a highly-oriented, very thin adsorbed film. Addition of approximately 1 sulfide attachment point per 100 backbone units results in a much thicker film, with large loops and a higher proportion of physisorbed chain segments than for the polymer derivatized with 1 sulfide per 10 backbone units. For both polymers, the sulfide side chains are distributed uniformly throughout the film thickness.

Adsorption Kinetics. The primary methods used to measure the kinetics of adsorption were ellipsometry and contact angle measurements. Without an independent measure of the amount of adsorbed material, changes in layer density cannot be distinguished from changes in layer thickness, particularly for flexible polymer molecules. Thus, the extent to which a material has approached the "equilibrium" value should be taken only as a measure of its proximity to the final state of thickness and coverage. A second issue is whether the thickness increases are

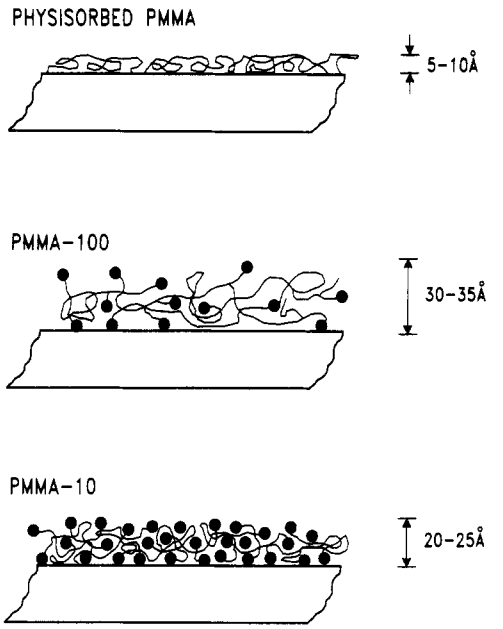

Figure 5. Schematic diagram of physisorbed and chemisorbed PMMA on a surface. Solid dots in the latter case represent sticky side chains containing sulfide groups.

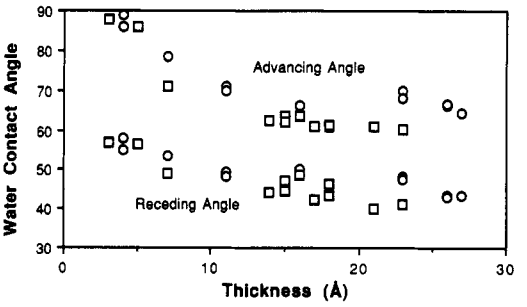

Figure 6. Water contact angle versus ellipsometrically measured film thickness for PMMA-10 (□) and PMMA-100 (○) adsorbed onto gold. The contact angle becomes independent of thickness beyond about 15 Å.

showing uniformly increasing layer thickness or the growth of islands. We have attempted to address this question by plotting water contact angles as a function of measured thickness (Figure 6). The variation in contact angles with observed film thickness suggests that the surface is only partially covered up to "thicknesses" of 15 Å. Above 15 Å, the water contact angles appear insensitive to further increases in measured thickness, suggesting that the initially-formed patches have merged to provide relatively complete coverage of the surface.

Ellipsometric measurements of the kinetics of adsorption for PMMA-10 and PMMA-100 are shown in Figure 7. Adsorption from the 0.001 mg/mL solutions is slow initially, but thicknesses at 130 h (points not shown on graph) do not increase significantly beyond the 48-h values. The 0.1 mg/mL solutions come to a nearly equilibrium value very quickly (the first three time points are 1, 10, and 60 min), with the measured thickness changing little up to 48 h. A plot of the measured thickness against the square root of time (Figure 8) shows that the two low concentration solution films have nearly identical straight line profiles for the first few hours. This indicates that adsorption is diffusion limited for these solutions; i.e., adsorption occurs faster than molecules can diffuse to the surface. Such diffusion-limited adsorption can be de-

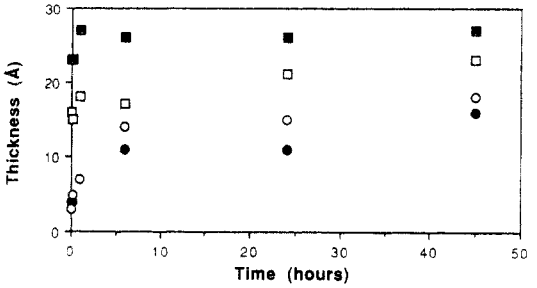

Figure 7. Kinetic changes in ellipsometric film thickness for adsorption of S-PMMA onto gold from solution in methyl ethyl ketone. Symbols: PMMA-100, (■) 0.1 and (●) 0.001 mg/mL; PMMA-10, (□) 0.1 and (○) 0.001 mg/mL.

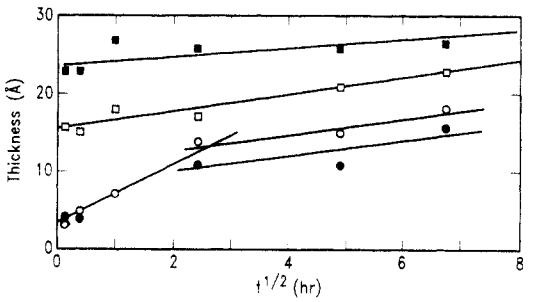

Figure 8. Kinetics of adsorption of S-PMMA films plotted versus the square root of time. Symbols same as in Figure 7.

scribed by the equation[18]

$$\Gamma_s(t) = 2C_0(Dt/\pi)^{1/2}$$

where Γ_s is the adsorbed amount per unit area, C_0 is the bulk concentration, D is the diffusion coefficient, and t is time. Since Γ_s can be represented as ρd, where ρ is the density of the film and d is the thickness, a plot of d vs $t^{1/2}$ will yield a straight line of slope $(2C_0/\rho)(D/\pi)^{1/2}$. The similarity in rate for PMMA-100 and PMMA-10 is expected in this case, since both are approximately the same molecular weight and should have about the same size and diffusion coefficient. Assuming the film has a density similar to that of PMMA (~1.2 g/cm^3),[14] the diffusion coefficient is calculated to be 5×10^{-7} cm^2/s, comparable to reported values of 7.2×10^{-7} cm^2/s for PMMA (MW = 79 000) in ethyl acetate and 6.8×10^{-7} cm^2/s for PMMA (MW = 201 000) in acetone.[15]

The lower ultimate film thicknesses formed from low-concentration solutions can be understood by considering the microscopic details of the adsorption process. Once a polymer molecule is in the proximity of the surface, two different polymer–surface interactions are important: the strong, specific attachment of the sulfide-derivatized side chains to the gold substrate (chemisorption) and the weaker, less specific interaction of the underivatized PMMA segments with the gold surface (physisorption). Polymer–polymer and polymer–solvent interactions are also important and may lead to displacement of weakly-bound chains. Strong Au–S linkages serve to pin the polymer molecule at the surface and increase interactions of the nearby underivatized chain segments with the metal surface. When diffusion to the surface is slow, the adsorbed molecules have time to spread on the surface via physisorption of adjacent segments and form more strong attachments. At low solution concentrations, both polymers yield layers of similar thickness, with the PMMA-100 layers perhaps a bit thinner. This may be explained by the supposition that higher concentrations of these tight attachments actually constrain the ability of the chain to spread across the surface. PMMA-100, with fewer strong anchor points, has more freedom to spread across the surface and thereby form a thinner film. But the increased proportion of physisorbed chain segments also produces a reduced ability of the molecules to bind strongly to an area already covered and to prevent other molecules from displacing the adsorbed chain. This point will be important in later discussions of secondary adsorption.

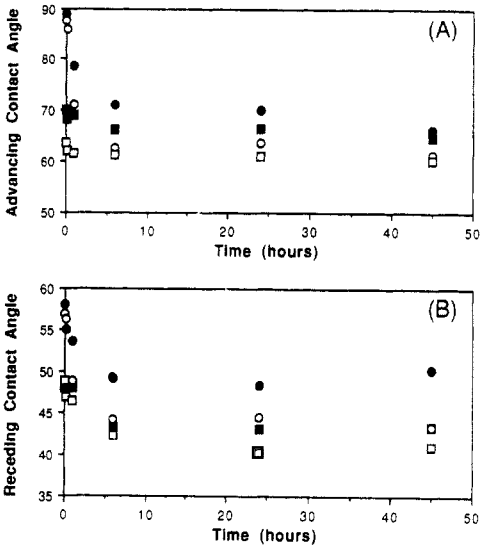

Figure 9. Water contact angle for S-PMMA films on gold as a function of adsorption time: (A) advancing contact angle; (B) receding contact angle. Symbols same as in Figure 7. Clean gold slides had θ_{adv}, $\theta_{rec} < 10°$. Gold slides in solvent for 24 h had $\theta_{adv} = 83 \pm 5°$, $\theta_{rec} = 47 \pm 4°$.

For thick films, the layer thickness is greater for PMMA-100, which has only 5–10 attachments per polymer chain as opposed to 50–80 for PMMA-10. When diffusion to the surface is fast compared to the rate of adsorption, the chains have little time to spread on the surface before any bare area around them is occupied by other molecules. Since PMMA-100 has so few tight attachment points per polymer chain, the likelihood for a part of the molecule which comes into contact with the bare surface to form a strong attachment and preclude displacement is much less than for PMMA-10. Thus, a plausible explanation for thinner layers of PMMA-10 at high concentrations results from the ability of the molecules to attach themselves more quickly to a greater amount of surface area than PMMA-100.

Variations in water contact angle with adsorption time add more insight into the structure of the adsorbed layers. Advancing contact angles approach equilibrium quickly for layers from 0.1 mg/mL solutions (Figure 9A). The values change by only a few degrees after the first minute. Contact angles of films formed from 0.001 mg/mL solutions have kinetic behavior similar to that seen with ellipsometry, coming close to equilibrium in about 6 h. Receding contact angles (Figure 9B) reach a steady value for all films after about 6 h of adsorption. There is more hysteresis in all cases than is observed for PMMA alone, and it is slightly greater for the thick films with both polymers. This seems unlikely to be due to increases in roughness or heterogeneity due to the fast coverage of the surface (such effects would be expected to be even greater in the films from short times) and may be due to increased mobility of the longer loops comprising the thicker films. Contact angles are also lower on PMMA-10, an effect we attribute to the presence of the large number of sulfide side chain groups which are not bound to the gold surface and may be present in a small concentration at the polymer–water interface.

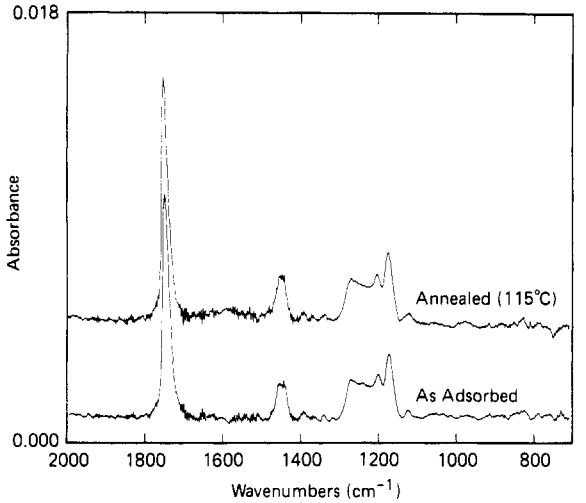

Figure 10. Infrared spectra ($E_\perp$) of a 32-Å-thick adsorbed layer of PMMA-100 before and after annealing for 16 h at 115 °C. The film is stable under these conditions and no significant difference is observed.

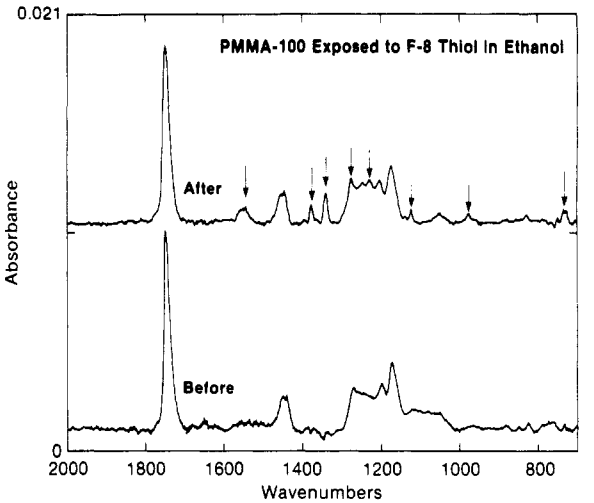

Figure 11. Infrared spectrum ($E_\perp$) of a PMMA-100 layer adsorbed to gold before and after exposure to a 10^{-4} M solution of F8-thiol. The peaks due to F8-thiol, marked by arrows, are clearly visible in the spectrum after exposure.

Thermal Response. Several films were annealed for 16 h at 115 °C (T_g for PMMA is 105 °C) in an attempt to allow more of the sulfide groups to attach to the surface and induce ordering in the films. According to the XPS results in Table II, there was little effect. Infrared spectra of films before and after annealing (Figure 10) are essentially identical. Interestingly, initial ellipsometric measurements indicated that the film thickness decreased upon annealing. The inconsistency of this result with the infrared and XPS measurements prompted further investigation. Comparison of the thickness of annealed films to the thickness of freshly adsorbed films on preannealed gold showed that the thickness did not change on annealing, in agreement with infrared and XPS results. The misleading initial ellipsometry results were thus traced to thermally-induced changes in the optical constants of the gold substrates. The observed shifts in the gold optical constants are consistent with a decrease in the roughness of the surface, similar to effects seen with other materials,[19-21] but more dramatic considering the mild conditions. XPS measurements of annealed gold detected no chromium at the surface. Contact angle measurements of annealed films were inconclusive because of considerable variability, perhaps due to low levels of contamination introduced during the many processing steps of annealing and analysis. The composite results of all measurements suggest that the surface organization achieved during 24 h of adsorption is stable to prolonged exposure to elevated temperature.

Secondary Adsorption. In an effort to determine the degree of substrate coverage and attachment of the S-PMMA chains, films were exposed to solutions of the fluorinated thiol, $F(CF_2)_8C(O)N(H)(CH_2)_2SH$ (F8-thiol), which itself self-assembles to form uniform monolayers.[22] The distinct positions of the infrared absorption bands arising from the fluorinated portion of the F8-thiol allow determination of the amounts of both F8-thiol and S-PMMA present on the surface after secondary adsorption (Figure 11). The amount of polymer displaced and the amount of F8-thiol which adsorbed onto the surface were measured after exposure to F8-thiol solutions in CH_2Cl_2 (a solvent for the polymers) and in ethanol (a nonsolvent for the polymers). Measurements of polymer loss were also made for exposure to each pure solvent.

For polymer displacement due to solvent alone, infrared measurements are summarized in Table III while ellipsometric estimates are shown in Table IV. For PMMA-100, the ellipsometric changes are only slightly smaller than the losses measured by infrared intensities. For PMMA-10, the ellipsometric results show a slight increase in film thickness in all cases of exposure to solvent. As expected, more polymer left the surface upon exposure to the better solvent CH_2Cl_2. The amount of polymer removed by solvent alone was much greater for PMMA-100, consistent with the PMMA-10 chains being bound to the surface at many more points than chains of PMMA-100 and therefore being more resistant to displacement. Exposure to F8-thiol had little effect on the amount of polymer lost from PMMA-10 layers, while a significantly greater amount of polymer was removed from the PMMA-100 layers in the presence of the F8-thiol.

Subtraction of the S-PMMA spectrum from the combined spectrum yielded a result that is very similar to the spectrum for a pure F8-thiol monolayer on gold (Figure 12), indicating that the F8-thiol is indeed present as an oriented, chemisorbed layer. Inaccurate subtraction in the polymer carbonyl stretch region occurs for thick polymer films, accompanied by the appearance of a peak near 1630 cm^{-1}. This is perhaps indicative of some F8-

Table III
Percentage of Polymer Lost As Determined by Infrared Measurements[a]

	PMMA-100		PMMA-10		PMMA
	ethanol	CH_2Cl_2	ethanol	CH_2Cl_2	CH_2Cl_2
exposure to solvent					
thick layer	3	40	6	14	0
thin layer	0	33	0	19	
exposure to F8-thiol					
thick layer	11	47	2	15	28
thin layer	12	50	0	14	

[a] Losses measured by changes in the intensity of the 1740-cm^{-1} band.

Table IV
Percentage of Polymer Lost upon Exposure to Solvent As Determined by Ellipsometry

	PMMA-100		PMMA-10		PMMA
	ethanol	CH_2Cl_2	ethanol	CH_2Cl_2	CH_2Cl_2
thick layer	0	35	0[a]	0[a]	0
thin layer	0	24	0[a]	0[a]	

[a] Film thicknesses increased after solvent exposure.

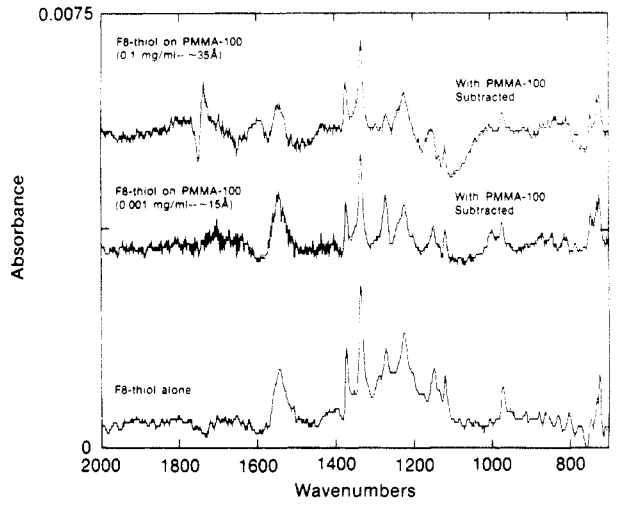

Figure 12. Comparison of reflection ($E_\perp$) infrared spectra of F8-thiol layers formed on PMMA-100-covered gold (polymer spectrum subtracted) with that of a pure monolayer of F8-thiol formed on gold.

Table V
Percentage of F8-thiol Monolayer Present after Secondary Exposure of S-PMMA Films[a]

	PMMA-100		PMMA-10	
	ethanol	CH_2Cl_2	ethanol	CH_2Cl_2
thick layer	66	76	45	60
thin layer	71	86	60	67

[a] Intensities of 1374- and 1336-cm^{-1} bands of F8-thiol layers formed on gold containing S-PMMA measured as a percentage of the intensity for pure F8-thiol monolayers on gold.

thiol being trapped in the S-PMMA layer, tied to the polymer side chains through hydrogen-bonding interactions rather than directly to the gold surface. This effect may alternatively arise from reorientation of the polymer chains in response to swelling by the secondary adsorption solvent. Such orientation changes induced by film swelling may account for the slightly higher polymer losses measured by infrared carbonyl intensities compared to the ellipsometric results as well as the increased film thicknesses for PMMA-10 as measured by ellipsometry. Estimates of the amount of F8-thiol adsorbed compared to the pure F8-thiol monolayer were made using the intensities of the 1336-, 1374-, and 1540-cm^{-1} absorption bands (Table V). The data can be quickly summarized by three observations. (1) About 10–20% more F8-thiol adsorbed onto a surface with a thin S-PMMA film than with a thick film, for both solvents. (2) About 10–20% more F8-thiol adsorbed onto the samples when using CH_2Cl_2 as a solvent compared with ethanol as the solvent. (3) Even with the most protected surface (a thick PMMA-10 layer) and with ethanol as the solvent, the infrared intensities of the F8-thiol layer are still nearly half those for a complete, pure F8-thiol monolayer on gold. This leads to the question of whether the F8-thiol is simply penetrating through the swollen adsorbed polymer layer to find bare gold or more actively displacing weakly attached sections of polymer chains at the surface. The displaced polymer may or may not leave the surface, depending on whether it is anchored in other places.

Contact angle measurements were employed to help answer these questions. Both advancing and receding contact angles were unchanged upon exposure of the S-PMMA films to solvent alone, even in those cases in which significant loss of adsorbed material was seen by infrared and ellipsometric measurements. For the thin

Table VI
Advancing Water Contact Angle (deg) after Exposure of S-PMMA Layers to a Solution of F8-thiol

	PMMA-100		PMMA-10	
	ethanol	CH_2Cl_2	ethanol	CH_2Cl_2
thick layer	91 ± 1	92 ± 1	66 ± 3	76 ± 3
thin layer	98 ± 2	97 ± 2	87 ± 2	91 ± 1

layers of underivatized PMMA and S-PMMA, it was expected that both the advancing and receding water contact angles would be affected by F8-thiol adsorption, since the thickness of these layers (<10 and ~15 Å, respectively) is of the same order as the ellipsometrically measured thickness of F8-thiol layers (~18 Å). For the underivatized PMMA, advancing and receding water contact angles after exposure to F8-thiol were 104 ± 6 and 65 ± 3°, compared to 68 ± 1 and 55 ± 2° before exposure. Comparison with the measured values of 114 ± 2 and 106 ± 2° for a pure F8-thiol monolayer on gold indicates that this ultrathin underivatized film is susceptible to secondary adsorption and that the fluorinated thiol chains are accessible at the film surface.

Changes in the advancing water contact angles were observed after exposure of the S-PMMA films to F8-thiol (Table VI), although receding contact angles remained essentially unchanged in all of the derivatized polymer systems. It appears that the F8-thiol does indeed protrude above thin S-PMMA layers, as seen from the fact that the advancing water contact angle on the thin PMMA-10 layer after ethanol treatment with F8-thiol (where none of the adsorbed polymer appeared to have been displaced from the surface) is nearly 90°. Surprisingly, the receding contact angle for the PMMA-100 layer after exposure to F8-thiol in CH_2Cl_2 is essentially unchanged from PMMA-100 alone, although nearly 50% of the polymer was lost and an F8-thiol signal of nearly 80% of that for a full monolayer is observed. These surfaces both appear to demonstrate some flexibility and ability to respond to the moving water front and fit the adage that the advancing contact angle is sensitive to the hydrophobic component of the surface energy (resistance to water spreading), while the receding contact angle is sensitive to the hydrophilic component of the surface energy (resistance to retraction of water).

The ability of the F8-thiol to penetrate the polymer layers without necessarily forming segregated thiol surface domains appears to be demonstrated for the thick PMMA-10 layer exposed to F8-thiol in ethanol. Although the F8-thiol signal is nearly half that for a full monolayer, the advancing and receding water contact angles are essentially unchanged from the values for the film prior to secondary adsorption. Almost no polymer is displaced, and apparently the thickness of the polymer film (~25 Å) is sufficient to completely shield the F8-thiol from the polymer–water interface. However, when the better solvent CH_2Cl_2 is used, some polymer leaves the surface, resulting in incomplete shielding as measured by a slight increase in advancing contact angle. For thick PMMA-100 layers, contact angles over 90° are obtained for both thick and thin films in both solvents, where polymer displacements range from 10% to nearly 50%. The inability of the PMMA-100 polymer to shield the F8-thiol from the polymer–water interface may be due to the greater displacement of chain segments from the surface because of fewer strong attachment points. The formation of segregated thiol surface domains is very likely in this case, since the thicker PMMA-100 layers would otherwise be expected to shield the adsorbed F8-thiol even more effectively than PMMA-10.

The F8-thiol appears to interact with the gold surface both by penetrating into the polymer layers and by displacing sections of chains from the surface. The polymer films appear to be relatively porous, since even the layer expected to be most resistant to penetration shows significant F8-thiol adsorption, although the layer remains intact enough to completely shield the F8-thiol during contact angle measurements. Displacement of chains seems to be a more important effect with PMMA-100, which has fewer points of attachment to the surface. However, even when a significant number of chains or chain sections have been displaced from the surface, these chains are able to interact with a water droplet strongly enough to give receding contact angles nearly identical to those of a similar polymer film with no F8-thiol.

Conclusions

The use of PMMA-based polymers with sulfur-derivatized side chains is a means of producing thin, tightly-attached films of polymers on gold. These films appear to be stable even upon prolonged exposure to temperatures above the T_g of PMMA. Both the thickness of the adsorbed films and their resistance to displacement depend on the concentration of the derivatized side chains. At low concentrations, where adsorption is diffusion limited, the two polymers produced films of similar thicknesses, but at higher concentrations films of PMMA-100 are thicker, presumably due to the ability of the PMMA-10 chains to attach more quickly to the surface. Films of PMMA-100 are also more easily depleted by exposure to solvent and are displaced by exposure to a fluorinated thiol, an effect not seen with the PMMA-10 films. PMMA-10 films also appear to be slightly oriented. A thick PMMA-10 film is still quite porous to the fluorinated thiol but retains enough integrity to completely shield the presence of F8-thiol during contact angle measurements.

XPS and contact angle measurements indicate that not all of the derivatized side chains react with the surface but that many appear to be distributed throughout the film thickness. This can be attributed to the significant steric constraints and loss of entropy which would have to be overcome in order for all sulfide-derivatized side chains to come into contact with the surface. Recent simulations by Tirrell et al.[23] have shown that three regimes of surface interaction with polymer chains can occur depending on the strength of interaction of the sticky segments. In the intermediate regime, these segments are found distributed throughout the thickness of the film as has been observed in this work. This raises the possibility that the presence of these untethered reactive chains may be used as the basis of further site-specific chemical reactions.

Acknowledgment. We thank Delores Miller of the IBM Almaden Research Center for assistance with the XPS analysis. We also thank Dr. C. Grant Willson of IBM for helpful discussions. Financial support was provided by IBM Endicott and by a Shared University Research agreement between IBM and the University of Mainz. L.H. thanks the Alexander von Humboldt Foundation for a Feodor Lynen Research Fellowship.

References and Notes

(1) Nuzzo, R. G.; Allara, D. L. *J. Am. Chem. Soc.* **1983**, *105*, 4481.
(2) Porter, M. D.; Bright, T. B.; Allara, D. L.; Chidsey, C. E. D. *J. Am. Chem. Soc.* **1987**, *109*, 3559.
(3) Bain, C. D.; Troughton, E. B.; Tao, Y.-T.; Evall, J.; Whitesides, G. M.; Nuzzo, R. G. *J. Am. Chem. Soc.* **1989**, *111*, 321.
(4) Ulman, A. *An Introduction to Ultrathin Organic Films from Langmuir–Blodgett to Self-Assembly*; Academic Press, Inc.: Boston, 1991.
(5) Bain, C. D.; Whitesides, G. M. *J. Am. Chem. Soc.* **1989**, *111*, 7164.
(6) Creager, S. E.; Collard, D. M.; Fox, M. A. *Langmuir* **1990**, *6*, 1617.
(7) Gomez, M.; Li, J.; Kaifer, A. E. *Langmuir* **1991**, *7*, 1797.
(8) Coyle, L. C.; Danilov, Y. N.; Juliano, R. L.; Regen, S. L. *Chem. Mater.* **1989**, *1*, 606.
(9) Häussling, L.; Michel, B.; Ringsdorf, H.; Rohrer, H. *Angew. Chem., Int. Ed. Engl.* **1991**, *30*, 569.
(10) Stouffer, J. M.; McCarthy, T. J. *Macromolecules* **1988**, *21*, 1204.
(11) Hofmann, V. Dissertation, University of Mainz, 1972.
(12) Greenler, R. G. *J. Chem. Phys.* **1966**, *44* (1), 310.
(13) Rabolt, J. F.; Jurich, M.; Swalen, J. D. *Appl. Spectrosc.* **1985**, *39*, 269.
(14) Smith, T. *J. Colloid Interface Sci.* **1980**, *75*, 51.
(15) *Polymer Handbook*, 3rd ed.; Brandrup, J., Immergut, E. H., Eds.; J. Wiley and Sons: New York, 1989.
(16) Havriliak, S.; Roman, N. *Polymer* **1966**, *7*, 387.
(17) Fadley, C. S. *Prog. Surf. Sci.* **1984**, *16*, 275.
(18) Carslaw, H. S.; Jaeger, J. C. *Conduction of Heat in Solids*, 2nd ed.; Oxford University Press: Oxford, 1959.
(19) Kono, S.; Hanekamp, L. J.; Van Silfhout, A. *Surf. Sci.* **1977**, *65*, 633.
(20) Chan, E. C.; Marton, J. P.; Brown, J. D. *J. Vac. Sci. Technol.* **1976**, *13* (4), 981.
(21) Fenstermaker, C. A.; McCrackin, F. L. *Surf. Sci.* **1969**, *16*, 85.
(22) Lenk, T. J.; Hallmark, V. M.; Rabolt, J. F.; Castner, D. G.; Erdelen, C.; Ringsdorf, H., manuscript in preparation.
(23) Konstandinidis, K.; Prager, S.; Tirrell, M. *J. Chem. Phys.* **1992**, *97*, 7777.